In-cloud processes of methacrolein under simulated conditions – Part 2: Formation of secondary organic aerosol

Imad El Haddad, Yao Liu, L. Nieto-Gligorovski, Vincent Michaud, Brice Temime-Roussel, Etienne Quivet, Nicolas Marchand, Karine Sellegri, Anne Monod

Atmos. Chem. Phys., 9, 5107–5117, 2009
www.atmos-chem-phys.net/9/5107/2009/

Atmospheric Chemistry and Physics

In-cloud processes of methacrolein under simulated conditions – Part 2: Formation of secondary organic aerosol

I. El Haddad[1], Yao Liu[1], L. Nieto-Gligorovski[1], V. Michaud[2], B. Temime-Roussel[1], E. Quivet[1], N. Marchand[1], K. Sellegri[2], and A. Monod[1]

[1]Universités d'Aix-Marseille I, II et III – CNRS, UMR 6264: Laboratoire Chimie Provence, Equipe: IRA, 3 place Victor Hugo, 13331 Marseilles Cedex 3, France
[2]Laboratoire de Météorologie Physique (UMR 6016), Observatoire de Physique du Globe de Clermont-Ferrand, Université Blaise Pascal, 24 avenue des Landais, 63177 Aubière, France

Received: 22 January 2009 – Published in Atmos. Chem. Phys. Discuss.: 10 March 2009
Revised: 19 June 2009 – Accepted: 24 June 2009 – Published: 28 July 2009

Abstract. The fate of methacrolein in cloud evapo-condensation cycles was experimentally investigated. To this end, aqueous-phase reactions of methacrolein with OH radicals were performed (as described in Liu et al., 2009), and the obtained solutions were then nebulized and dried into a mixing chamber. ESI-MS and ESI-MS/MS analyses of the aqueous phase composition denoted the formation of high molecular weight multifunctional products containing hydroxyl, carbonyl and carboxylic acid moieties. The time profiles of these products suggest that their formation can imply radical pathways. These high molecular weight organic products are certainly responsible for the formation of secondary organic aerosol (SOA) observed during the nebulization experiments. The size, number and mass concentration of these particles increased significantly with the reaction time: after 22 h of reaction, the aerosol mass concentration was about three orders of magnitude higher than the initial aerosol quantity. The evaluated SOA yield ranged from 2 to 12%. These yields were confirmed by another estimation method based on the hygroscopic and volatility properties of the obtained SOA measured and reported by Michaud et al. (2009). These results provide, for the first time to our knowledge, strong experimental evidence that cloud processes can act, through photooxidation reactions, as important contributors to secondary organic aerosol formation in the troposphere.

Correspondence to: I. El Haddad
(imad.el-haddad@etu.univ-provence.fr)

1 Introduction

Isoprene accounts for about half of all volatile organic compounds (VOC) emissions in the atmosphere and is, on a mass basis, the dominant emitted biogenic VOC with an average global emission of 410 Tg yr^{-1} (Müller et al., 2008). Its contribution to SOA budget was believed to be negligible until very recently when heterogeneous pathways were investigated. In this manner, Claeys et al. (2004a, b) measured significant concentrations of tetrols and related species in ambient particle matter, and provided strong evidence that these compounds were formed during the oxidation of isoprene and its first generation oxidation products such as methacrolein. Furthermore, several smog chamber experiments investigated the SOA formation from isoprene, and reported yields of 1–4% (Edney et al., 2005; Dommen et al., 2006; Kroll et al., 2006; Surratt et al., 2006). They suggested that isoprene and its oxidation products (methacrolein, 3-methylfuran…) can contribute to ambient SOA via heterogeneous reactions under acidic conditions or via polymerization of second generation oxidation products. Accordingly, Surratt et al. (2006) demonstrated a major contribution of methacrolein in the SOA formation through isoprene reactivity, and proposed particle phase esterification as a major SOA formation pathway. With a global emission rate of 410 Tg yr^{-1}, isoprene is believed to produce, through heterogeneous pathways, substantial amounts of SOA even with low SOA yields (Kanakidou et al., 2005). However, these mechanisms do not take into account those occurring through cloud processes.

Published by Copernicus Publications on behalf of the European Geosciences Union.

Clouds play a major role in atmospheric chemistry, because they strongly affect the chemical composition of the troposphere. The cloud droplets provide an efficient medium for liquid phase reactions of water soluble species, and more than 60% of the total sulfates on a global scale are estimated to be produced from cloud processing (Liao et al., 2003). Recent studies suggest that, as sulfates, SOA can also be produced through aqueous phase reactions in clouds, fogs and aerosol water (Blando and Turpin, 2000; Ervens et al., 2003, 2004a, b, 2008; Gelencser and Varga, 2005; Lim et al., 2005; Altieri et al., 2006, 2008; Carlton et al., 2006, 2007). Briefly, reactive organics are oxidized in the interstitial spaces of clouds to form highly water-soluble compounds (e.g. aldehydes) that readily partition into the droplets. The dissolved organics may undergo chemical conversions in the aqueous phase (hydrolysis, further oxidation, polymerization…), to form less volatile organics. These products remain, at least in part, in the particle phase upon droplet evaporation, leading to SOA mass production (Kanakidou et al., 2005). The results obtained from several experimental studies support the in-cloud SOA hypothesis. Loeffler et al. (2006) demonstrated the formation of SOA through the self-oligomerization of glyoxal and methylglyoxal, when aqueous solutions of these products were evaporated. Likewise, photochemical experiments conducted on pyruvic acid, methylglyoxal, and glyoxal clearly demonstrated the formation of higher mass products that can potentially participate in SOA production, upon cloud droplets evaporation (Altieri et al., 2006, 2008; Guzmann et al., 2006; Carlton et al., 2006, 2007). Based on these findings, Ervens et al. (2008) have developed a cloud parcel model that supported in-cloud SOA (called SOA_{cloud}) formation from isoprene and its oxidation products, and they obtained a carbon yield of SOA_{cloud} ranging from 0.4 to 42%.

Methacrolein is a major gas phase reaction product of isoprene (Lee et al., 2005) that was observed in the gas phase and in cloud and fog waters (Van, Pinxteren et al., 2005). The aim of this study is to investigate the ability of methacrolein to form SOA after in-cloud aqueous phase photooxidation followed by droplets evaporation, and to determine the resulting SOA yield.

2 Experimental section

In order to investigate the fate of methacrolein in cloud water, photochemical aqueous-phase reactions of methacrolein with OH radicals were performed. The aqueous solutions obtained at different reaction times were then nebulized and dried into a mixing chamber, in order to simulate a cloud evaporation process. The number size distribution of the obtained SOA in the mixing chamber was tracked using a SMPS. The aqueous-phase composition was analyzed by ESI-MS/MS, in order to investigate the organic species implicated in the production of SOA through cloud processing.

2.1 Aqueous phase reaction

OH-oxidation of methacrolein was studied in an aqueous phase photoreactor (Liu et al., 2009). Briefly, it is a 450 mL Pyrex thermostated reactor, equipped with Xenon arc lamp (300 W; Oriel). The OH radicals were produced by H_2O_2 photolysis. The experiments were performed at 25°C and "free pH" (unbuffured solutions). The initial concentrations of methacrolein ($2–5\times10^{-3}$ M) and H_2O_2 (0.4 M) were representative of aerosol water conditions. The good reproducibility of aqueous phase OH-oxidation of methacrolein was verified through a series of 9 experiments (Liu et al., 2009). To reach the goals of the present study, a two additional experiments were performed under the same conditions, where samples were taken at 0 h, 5 h, 9.50 h, 14 h and 22 h for the aerosol generation experiments.

2.2 Analytical determinations

The ESI-MS and ESI-MS/MS analyses were conducted using a triple quadrupole mass spectrometer (Varian 1200L), equipped with an electrospray ionization (ESI) chamber. Samples and standard solutions were directly injected (no chromatographic column) into the ESI source region at a flow rate of 25 μL min^{-1}. Two experiments were performed using the coupling of the aqueous phase photoreactor with the mass spectrometer ESI source, following the procedure described in Poulain et al. (2007). The ESI-MS and ESI-MS/MS analysis were performed in both positive and negative modes using the conditions described in Liu et al. (2009).

In addition, samples taken at different reaction times were analyzed by HPLC-APCI-MS/MS (Varian 1200L). The separation column was a Synergi Hydro-RP 250×2.0 mm i.d. (4 μm), Phenomenex. The analytes were chromatographically resolved using a gradient of two solvents (A: 0.1% acetic acid aqueous solution and B: methanol) delivered at a constant flow rate of 0.2 mL min^{-1}, with A:B=95%:5% from 0 to 12 min and 0%:100% at 60 min during 5 min. The analysis was realized using single ion monitoring (SIM) in the negative and the positive ionization modes of the APCI, at −40 V and +40 V, respectively. The nebulizing gas was synthetic air for the negative mode and nitrogen for the positive mode. It was delivered at a pressure of 55 psi at a temperature of 300°C. Nitrogen served both as the drying gas and the auxiliary gas at a pressure of 15 and 3 psi, respectively. The temperature of the drying gas was held at 350°C.

2.3 Aerosol generation and characterisation

The experimental setup used for the aerosol generation experiments is presented in Fig. 1. Liquid samples, taken from the photoreactor at specific reaction times, were nebulized using a TSI 3079 atomizer, in order to generate submicrometer water droplets. The atomizer flow rate was fixed at 4.2 L min^{-1}. The generated water droplets were then dried

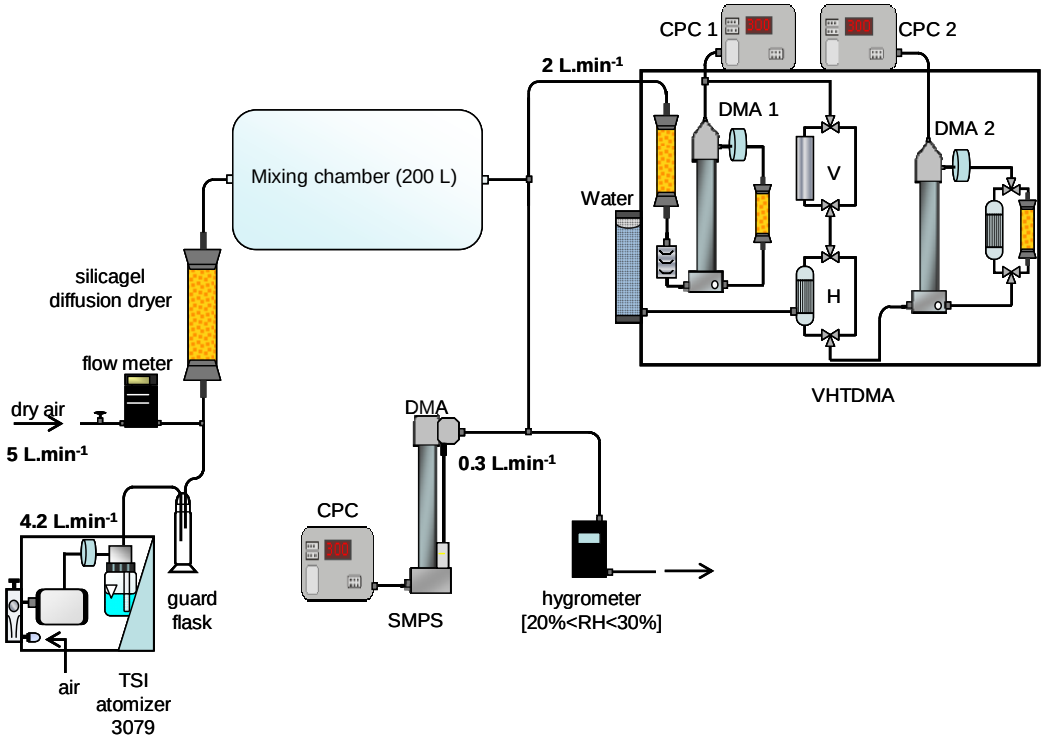

Fig. 1. Scheme of the experimental setup for aerosol generation.

by mixing with pure dry air at a flow rate of 5 L min^{-1} and passing through a silica gel diffusion dryer. After drying, the aerosol was delivered into a 200 L Teflon (PTFE) mixing chamber. At these operating conditions, the average residence time of the aerosol in the whole setup was about 20 min, and the resulting relative humidity was 20–30% in the mixing chamber (Fig. 1). The aerosols obtained at different aqueous phase reaction times were characterised in terms of their number size distributions, hygroscopicity and volatility. The size distribution of the generated aerosol was monitored using a Scanning Mobility Particle Sizer (SMPS) connected to the mixing chamber (Fig. 1). The SMPS is composed of a long column Differential Mobility Analyzer (L-DMA, GRIMM Inc.) and a Condensation Particle Counter (CPC, model 5.403, GRIMM Inc.). The DMA aerosol and sheath operating flow rates were 0.3 and 3 L min^{-1}, respectively. These settings allowed for a particle sampling range from 11.1 to 1083 nm, within 6 min 46 s. The aerosol hygroscopicity and volatility measurements were conducted using a Volatility Hygroscopicty Tandem DMA (HVTDMA) (Fig. 1). The experimental procedure and the results dealing with the latter measurements are reported in Michaud et al. (2009). Before each nebulization experiment, the mixing chamber was flushed for about 2 h (∼6 times) with synthetic air, and aerosol blanks were controlled by SMPS measurements prior to each new experiment.

During the nebulization of each aqueous solution, an increase of the aerosol mass by a factor of approximately two within 5 h was observed. Therefore, at each reaction time, an average particle size distribution and mass was calculated during 2 h of nebulization, starting after the first hour.

3 Results and discussion

3.1 Aqueous phase characterisation

As described in Liu et al. (2009), during the aqueous phase reaction, 70% of methacrolein was consumed within 10 h. Several reaction products were identified and quantified, including formaldehyde, formic acid, acetic acid, methylglyoxal, hydroxyacetone, oxalic acid, glyoxylic acid, methacrylic acid, peroxymethacrylic acid, 2-hydroxy-2-methylmalonaldehyde, 2,3-dihydroxy-2-methylpropanal, 2-methylglyceric acid, pyruvic acid and dihydroxymethacrylic acid. The chemical mechanism associated to these products is discussed in Liu et al. (2009). The authors reported a significant deficit in the carbon balance of up to 45%, which is related to unidentified reaction products. A thorough study of the ESI-MS spectra at different reaction times show a large number of high molecular weight ions in both the positive and the negative modes (Fig. 2), which can explain this deficit of carbon. The most abundant ions in both modes cluster in the mass range of 100–250 amu and some ions up

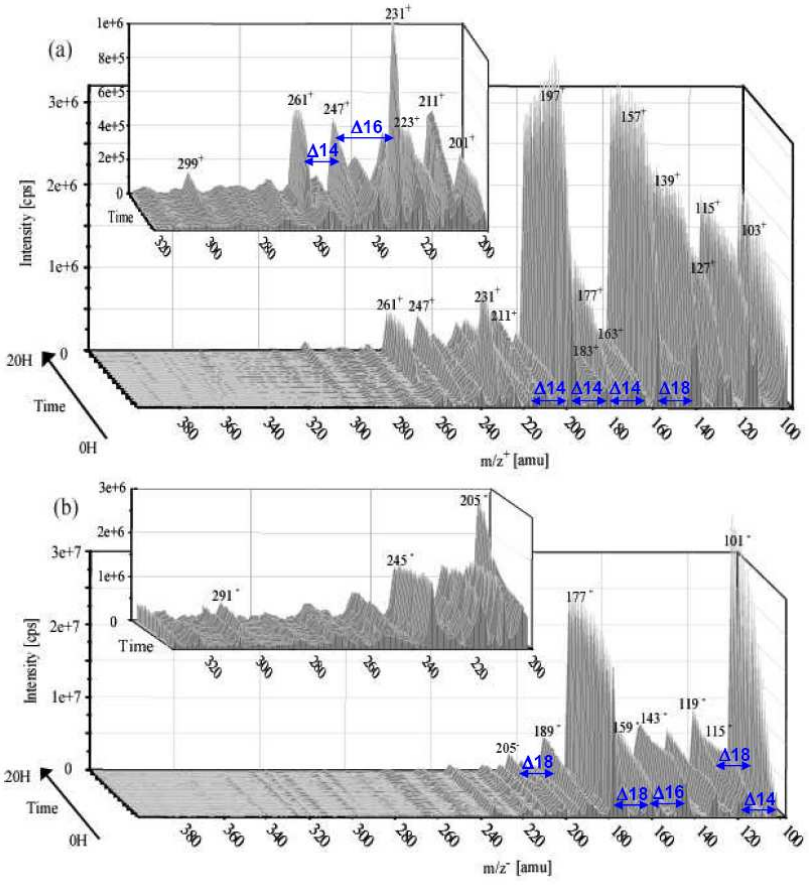

Fig. 2. 3-D time profiles of the mass spectra obtained by ESI/MS analysis from 100 to 400 amu, during the aqueous phase OH-oxidation of methacrolein. **(a)** in the positive mode **(b)** in the negative mode. For each mode, a zoom from 200 to 320 amu is shown.

to 320 amu are also observed. Over 400 amu no ions were observed under our instrumental conditions. Similar ESI-MS distribution patterns have been reported previously by Altieri et al. (2006, 2008), during the aqueous phase photooxidation of pyruvic acid and methylglyoxal. This distribution appears to be consistent with the development of an oligomer system that shows a highly regular pattern of mass differences of 12, 14, 16 and 18 amu (Altieri et al., 2006, 2008; Poulain et al., 2007). In the present study, Figure 3 shows that the observed ions were not detected in the spectra of standard mixtures containing methacrolein, formaldehyde, methylglyoxal, hydroxyacetone, formic, acetic, pyruvic, oxalic, glyoxylic and methacrylic acids, even at concentrations representative of the solution after 20 h of reaction. This suggests that the observed oligomer formation is not an analytical artifact occurring during the electrospray ionization, i.e. adducts formed in the ionization chamber by the combination of smaller molecules.

Figures 2 and 3 show the complex nature of the matrix and the complexity of the mechanisms behind the formation of these products. The complexity in the ESI-MS spectra occurs in both positive and negative modes, thus indicating that the oligomers formed in the aqueous phase are most likely multifunctional compounds. The observed MS compounds were further characterized for their MS/MS fragmentation in order to elucidate their chemical structures. The MS/MS patterns allowed us to group these compounds into two remarkable series: series A in the negative mode and series B in the positive mode (Table 1). In these series, each parent ion exhibits in its MS/MS spectra at least one daughter ion corresponding to another parent ion of the same series. This suggests that, in each series, the compounds associated to the parent ions include in their structure the same structural units, thus significantly denoting the formation of oligomers. For each series, the HPLC-APCI-MS analysis showed that the parent ions had different retention times, which attribute them to different reaction products. A detailed discussion of the HPLC-MS analysis of each series is presented hereafter.

– In series A (Fig. 4), the smallest ions, ($m/z\,73^-$ and 87^-) are related, respectively, to glyoxylic and pyruvic acids, which are secondary oxidation products of methacrolein (Liu et al., 2009). This series also exhibits two higher molecular weight ions, $m/z\,143^-$ and

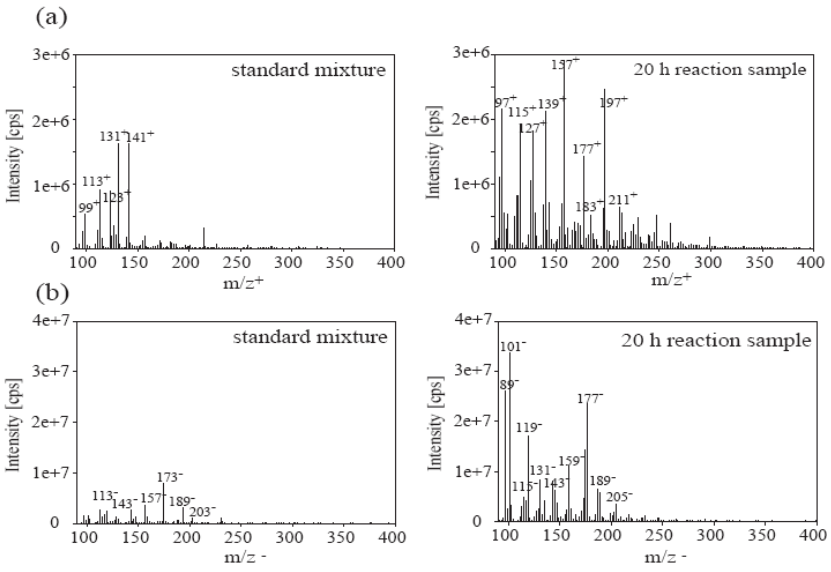

Fig. 3. Comparison of the mass spectra between the standard mixture and a sample after 20 h of reaction **(a)** in the positive mode **(b)** in the negative mode. The standard mixture contains methacrolein (3.10^{-3} M); formaldehyde, methylglyoxal, hydroxyacetone, formic and acetic acids (6.10^{-4} M) ; pyruvic, oxalic, glyoxylic and methacrylic acids (3.10^{-5} M).

Table 1. MS/MS fragmentations of some observed parent ions, in the negative (series A) and the positive mode (series B).

Ion series	parent ion (amu)[a]	Daughter ions[a]	Neutral losses[b]
negative mode			
A	187^{-}[d]	169^{-} 159^{-} $\mathbf{143}^{-}$ 125^{-} $\mathbf{87}^{-}$	18 28 44 56 62
	$\mathbf{143}^{-}$[d]	125^{-} 99^{-} 97^{-} $\mathbf{87}^{-}$ 85^{-} $\mathbf{73}^{-}$ 57^{-}	18 28 30 44 46 56
	$\mathbf{87}^{-}$ (pyruvic acid)[d]	43^{-}	44
	$\mathbf{73}^{-}$ (glyoxylic acid)[d]	45^{-}	28
positive mode			
B	201^{+}[c]	183^{+} 165^{+} $\mathbf{155}^{+}$ 95^{+}	18 28 36 46 60 70 88
	197^{+}[c]	179^{+} $\mathbf{109}^{+}$ 95^{+} 85^{+}	18 70 94 102
	173^{+}[c]	$\mathbf{155}^{+}$ 139^{+} $\mathbf{127}^{+}$ $\mathbf{109}^{+}$	18 28 30 46 64
	$\mathbf{155}^{+}$[c]	$\mathbf{137}^{+}$ $\mathbf{127}^{+}$ 113^{+} $\mathbf{109}^{+}$ 95^{+} 81^{+}	18 28 46 56 60 74
	$\mathbf{137}^{+}$[c]	$\mathbf{109}^{+}$ 95^{+} 81^{+} 43^{+}	28 56
	$\mathbf{127}^{+}$[c]	$\mathbf{109}^{+}$ 99^{+} 85^{+} 83^{+} 81^{+} 43^{+}	18 28 46 56
	$\mathbf{109}^{+}$[c]	81^{+} 79^{+}	28 30

[a] The ions in bold were observed both as parent ions (formed during the reaction) and daughter ions.
[b] Neutral losses can correspond to: 18 (H_2O); 28 (CO); 30 (HCHO); 36 ($2\times H_2O$); 44 (CO_2); 46 (H_2O+CO); 56 ($2\times$CO); 60 (CH_3COOH); 62 (CO_2+H_2O); 88 ($2\times CO_2$).
[c] Time profile corresponding to a primary reaction product.
[d] Time profile corresponding to a secondary or tertiary reaction product.

187^{-}. The chromatogram associated with *m/z* 187^{-} exhibits a sharp peak at 28.6 min and a smaller peak at a higher retention time (37.4 min) (Fig. 4b), thus corresponding to two different compounds having the same molecular mass of 188 g mol^{-1}. The collision-induced dissociation of *m/z* 187^{-} mainly leads to two predominant daughter ions at *m/z* 143^{-} and 87^{-} (Table 1). The *m/z* 143^{-} daughter ion, resulting from the loss of CO_2 as a neutral fragment (44 uma), indicates the presence of at least one carboxylic acid functional group (Dron et al., 2007). The *m/z* 87^{-} daughter ion suggests that at least one of the two products associated with *m/z* 187^{-} include in its chemical structure the pyruvate as a structural subunit. The HPLC-MS chromatogram

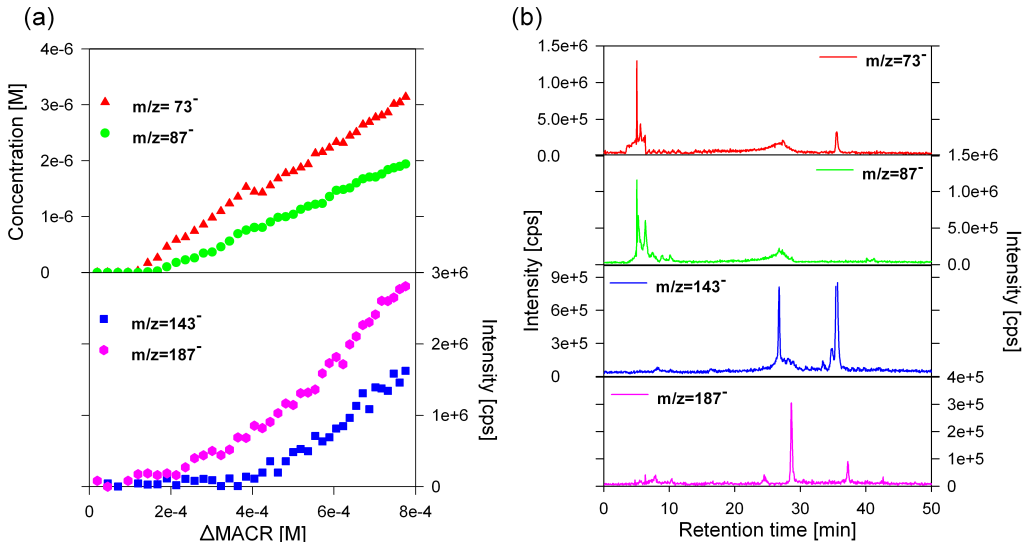

Fig. 4. Characteristics of the oligomer series A. **(a)** Evolution of the MS fragments intensities (143^- and 187^-) from the series A, along with the concentration of the glyoxilic (73^-) and the pyruvic acid (87^-). **(b)** HPLC chromatographic profiles of the corresponding fragments.

of *m/z* 143^- exhibits two peaks at 26.50 and 35.44 min (Fig. 4b), which can, also, be attributed to two different compounds. The MS/MS analysis of *m/z* 143^- exhibits, among others, daughter ions of *m/z* 73^- and 87^- thus denoting the presence of the glyoxylate or the pyruvate as a structural subunit. The MS/MS fragmentation patterns and the high retention times of *m/z* 143^- and 187^- of series A, clearly, associate them to high molecular weight multifunctional compounds, produced probably from the reaction of pyruvic acid. The contribution of pyruvic acid to the formation of oligomers through aqueous phase oxidation was previously observed by Altieri et al. (2006, 2008) and Guzman et al. (2006). However, it should be noted that these authors proposed different reaction pathways in order to explain the oligomer formation: Altieri et al. (2006, 2008) suggest molecular (esterification) additions of smaller compounds including pyruvic acid, glyoxylic acid, and oxalic acid; whereas Guzman et al. (2006) proposed a radical mechanism. In the present study, the data do not permit the determination of the reaction pathways for the products of series A.

– In series B (Fig. 5), the HPLC-MS chromatograms associated with the parent ions indicate that they are, apparently, related to a complex mixture of numerous compounds and isomers. The chromatograms of *m/z* 137^+, 155^+ and 173^+ exhibit more than five resolved peaks and a broad peak at a retention time of ∼27 min. The chromatograms associated with *m/z* 197^+ and 201^+ do not show any peak, which suggests that the corresponding compounds were not eluted under our conditions (Fig. 5). These chromatographic aspects can be attributed to the high molecular weight and the multifunctional nature of the compounds associated with this series. Likewise, the collision-induced dissociation of *m/z* 109^+, 127^+, 137^+, 155^+, 173^+, 197^+ and 201^+ frequently yields neutral losses of H_2O (18 uma), CO (28 uma), H_2O+CO (46 uma) and 2×CO (56 uma) (Table 1) which relate them to hydroxyl and carbonyl moieties (hydroxy-carbonyl or carboxylic acids) and confirm their multifunctional nature. The time profiles of the intensities of *m/z* 109^+, 127^+, 137^+, 155^+, 173^+, 197^+ and 201^+ as a function of consumed methacrolein (Fig. 5a) shows direct formation (with no time delay). This pattern indicates that the corresponding compounds are first generation (primary) products. In the present study, the fact that the oligomer series B corresponds to primary reaction products points out that the oligomer formation bypasses the primary stable oxidation products and includes only methacrolein as a reaction substrate. It is thus likely that the oligomerization mechanism leading to series B compounds proceeds via radical mechanisms in good agreement with the mechanism pathways proposed by Guzman et al. (2006), rather than ionic or molecular additions (such as esterification, aldol condensation, acetylation...). This mechanism occurs somehow through the combination of the radicals formed from the OH-oxidation of methacrolein with another methacrolein molecule or another first generation radical. The multiple additions of different primary radicals may explain the different first generation high molecular weigh products associated to the fragments observed in series B.

In series B, after ∼5 h of reaction, the intensity of most of the ions reached a plateau or started to decrease. This can be attributed to further reaction of the corresponding compounds, thus showing that the formed oligomers can be sensible to photochemistry. The degradation of higher mass compounds was previously observed during the aqueous phase OH-oxidation of glyoxal (Carlton et al., 2007). The authors suggested this degradation as a possible pathway for the formation of smaller non volatile organic acids, such as oxalic acid. Thus, these smaller compounds were secondary products, in good agreement with our observations in series A.

3.2 SOA formation

Considering the molecular mass range and the functionality of the aqueous phase products observed in Sect. 3.1, these compounds are believed to be particularly low volatile. The ability of these compounds to produce SOA upon water droplets evaporation was experimentally examined by nebulizing and drying the reaction samples, using the setup described in Fig. 1. The obtained SOA size distribution averages and standard deviations for each reaction time and the corresponding SOA total number, modal diameter, and particle mass (calculated assuming a particle density of 1 g cm^{-3}) are reported in Fig. 6 and Table 2. Because the obtained size distributions can depend on the nebulizer operating mode, only a relative change in the size distributions will be considered hereafter. The comparison between the particle size distributions obtained at different reaction times clearly shows a significant production of SOA (Fig. 6). At the initial reaction time (0 h), the aerosol size distribution was determined by nebulizing an aqueous mix of the reactants (methacrolein+H_2O_2). This experiment was repeated tree times and the generated aerosol showed an average mass concentration ($M_{0\,h}$) of 0.03±0.02 μg m^{-3} (Table 2), assuming a particle density of 1 g cm^{-3}. This concentration value was not statistically different from the one measured for the aerosol generated by nebulizing a pure water solution (18 MΩ cm^{-1}) (T-test 0.05 level; Sokal and Rohlf, 1981). These results support the fact that methacrolein is highly volatile, and thus, is not able to produce particles. After 5 h of aqueous phase reaction, the aerosol quantity was low ($M_{5\,h}$=1.4±0.3 μg m^{-3}), but significantly higher than $M_{0\,h}$. Between 05 h and 9.50 h, a substantial increase of the aerosol mass concentration was observed. After 14 h, the aerosol quantity increased steadily as a function of the aqueous-phase reaction time. At 22 h, the aerosol mass concentration reached 27.8±5 μg m^{-3}, about three orders of magnitude higher than the initial aerosol quantity. Similarly, a significant increase of the aerosol diameter and number was observed: from 0 to 22 h, the aerosol number and diameter have increased by a factor of 254 and 3.7, respectively (Table 2). This evolution clearly demonstrates the ability of the aqueous phase processes to produce particles upon water

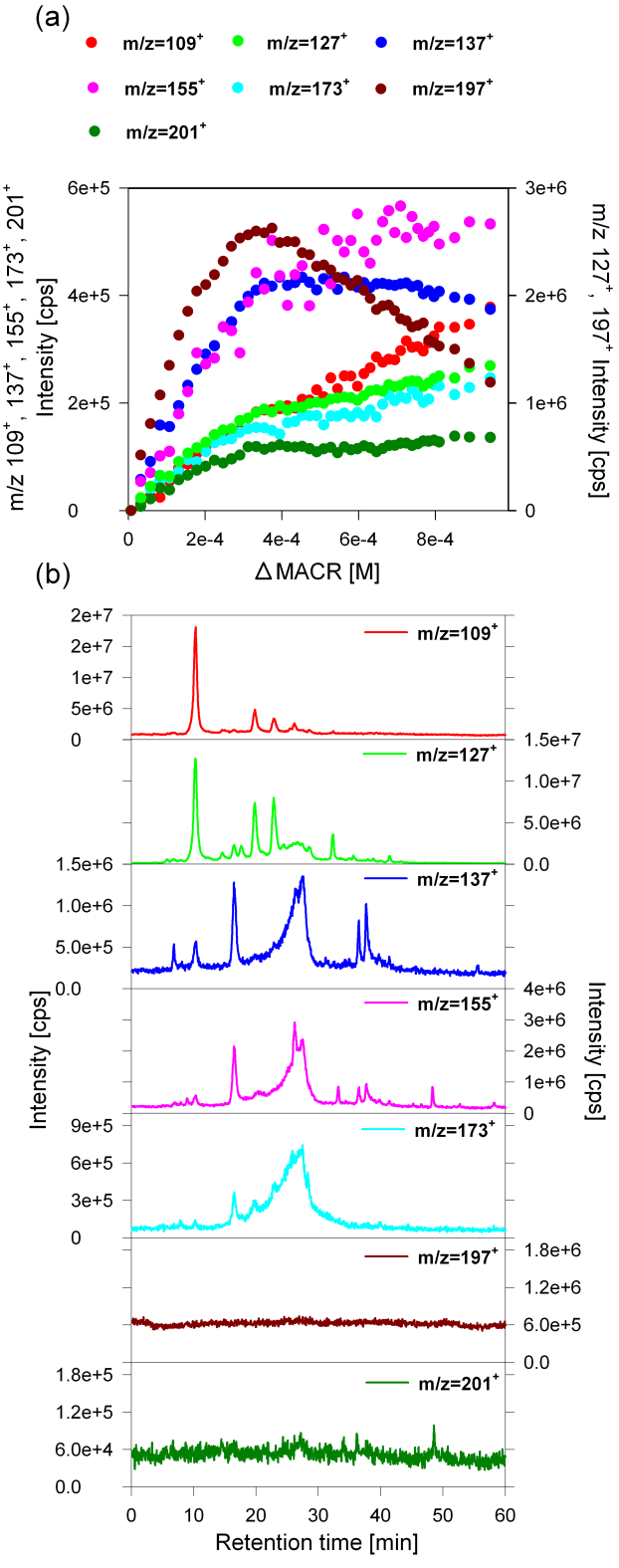

Fig. 5. Characteristics of the oligomer series B. **(a)** Evolution of the series B MS fragments intensities. The *m/z* 127$^+$ and 197$^+$ are plotted on the secondary axe. **(b)** HPLC chromatographic profiles related to the different MS fragments.

Table 2. Characteristics of the aerosol formed by the nebulization of the aqueous solutions obtained at different reaction times. The values reported are the average of multiple SMPS measurements, and the errors indicated are the standard deviation on these averages.

Reaction time	N[a] ($\times 10^3$ cm^{-3})	D_P^b (nm)	M[c] (μg m^{-3})	ΔMACR[d] (μg mL^{-1})	SOA[e] (μg mL^{-1})	Yield[f] (%)
0 h	1±4	13.4±1.7	0.03±0.02	0	0.04±0.01	0
5 h	45±7	17.3±3.8	1.4±0.3	130±13	1.87±0.70	1.6±0.7
9.50 h	163±30	41.1±2.1	10.5±2.2	205±21	14.3±4.9	7.6±3.1
14 h	205±22	46.1±2.4	17.5±3.3	254±25	23.8±8.1	10.2±4.2
22 h	254±20	49.8±3.3	27.8±5.0	304±30	32.7±11.1	11.7±5.3

[a] Total number of aerosol generated by the nebulization of the aqueous solutions obtained at different reaction times.
[b] Particle diameter mode.
[c] Aerosol mass concentration measured by the SMPS assuming a particle density of 1 g cm^{-3}.
[d] Methacrolein consummation during the aqueous phase reaction.
[e] SOA aqueous phase concentrations calculated using the SOA mass concentration determined by SMPS and the particles transmission efficiency evaluated by the nebulization of a NaCl aqueous solution at 100 mg L^{-1}.
[f] SOA yield calculated for each reaction time as the ratio of the SOA concentrations over the methacrolein consummation.

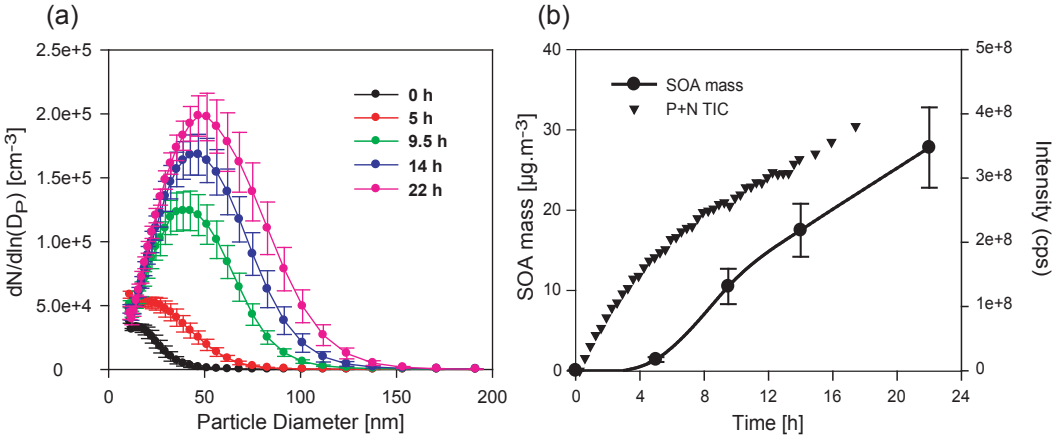

Fig. 6. (a) Evolution of the particle size number distributions of the generated SOA as a function of reaction time during the aqueous phase OH-oxidation of methacrolein. SOA was generated using the experimental setup described in Fig. 1. The particle number distributions of the generated SOA are an average of several distributions measured at the corresponding reaction times; the error bars represent the standard deviation of these averages. **(b)** Evolution of the SOA mass compared to the sum of the MS total ion current of the aqueous samples in the positive and the negative mode (P+N TIC) with the reaction time. The SOA mass are calculated using the SMPS data and assuming a particle density of 1 g cm^{-3}.

droplets evaporation. This production can be attributed to the low volatile organic species formed during the aqueous phase OH-oxidation of methacrolein (Sect. 3.1) which remain in the particle phase upon water evaporation, and thus forms the observed SOA. Among the products identified by Liu et al. (2009), several compounds such as dihydroxymetharylic acid (Claeys et al., 2004a, b) and oxalic acid (Sempéré and Kawamura, 1996; Kawamura and Sakaguchi, 1999) are low volatile compounds and can contribute at least in part to the SOA mass. Other products, such as methylglyoxal (also identified by Liu et al., 2009), were previously reported to potentially form low volatility compounds through reactive pathways during droplets evaporation and products accretion (Loeffler et al., 2006; Paulsen et al., 2006). Therefore, the occurrence of additional formation of high molecular weight products from smaller products, such as methylglyoxal, induced by water evaporation may contribute to the SOA mass. In addition, the unidentified high molecular weight multifunctional compounds are believed to be sufficiently low volatile to remain predominantly in the particle phase upon water droplets evaporation. Nevertheless, the contribution of each of these identified or unidentified products to the observed SOA cannot be evaluated because the chemical analysis of SOA was not performed in this work. Further investigations are thus needed, especially focussing on the chemical composition of SOA formed upon cloud droplet evaporation.

3.3 SOA mass yield and atmospheric implications

In order to determine the SOA mass yield, we evaluated first the particle losses in our experimental setup. This estimation was determined on the basis of four nebulization experiments of aqueous solutions containing NaCl at 100 mg L^{-1} using the experimental setup described in Fig. 1. Although particles transmission efficiencies can slightly differ between organic and inorganic particles, NaCl was chosen to estimate the transmission efficiencies of the setup for two reasons: i) NaCl is exclusively in the particulate phase which is not the case for most of the organic species; ii) Na^+ and Cl^- can be quantified with high level of precision in both water and aerosol phases. The results have shown that the particles transmission efficiency from our system was only 11.3±2.5%. This low efficiency may be due to the experimental set up which contains a guard flask and a small mixing chamber, made of Teflon, which is highly electrostatic. Assuming the same loss for organic particles, we used this value to evaluate the SOA mass yield. In this kind of experiments, the determined yields depend on several experimental parameters such as the reactant concentrations and the reaction time. This yield was calculated at each reaction time as the ratio between the amount of SOA formed in milligram per liter of evaporated water and the consumed methacrolein in milligram per liter of evaporated water (Table 2). The obtained amount of SOA (14–33 mg L^{-1} for reaction times 9.50–22 h) is in good agreement (within the uncertainties) with the values obtained by Michaud et al. (2009) (19–41 mg L^{-1} for the same reaction times) who performed an independent calculation based on volatility measurements, and which does not integrate the particle transmission efficiencies of the setup. The mass yields estimated here depend on the reaction time but a global yield of 2–12% can be assessed (Table 2). This global yield is higher than the 1–4% mass yield of SOA formed through direct photooxidation of isoprene in the gas phase, and thus, it should enhance the total mass of SOA formed from isoprene in the atmosphere. To evaluate more accurately the importance of these aqueous processes in SOA production in the troposphere, further works are still needed. In particular, the relevance of these processes has to be investigated considering methacrolein aqueous phase concentrations and reaction times consistent with those observed in cloud droplets.

4 Conclusions

This work reports an experimental study of the aqueous phase reaction of methacrolein with OH radicals, which is one of the major oxidant in the tropospheric aqueous phase. The fate of the obtained solutions was investigated upon water droplets evaporation. The aqueous phase reaction products were characterized using ESI-MS, ESI-MS/MS and HPLC-APCI-MS. Several low volatile compounds, such as oxalic acid and dihydroxymethacrilic acid, were formed along with other unidentified higher molecular weight multifunctional products. The HPLC-APCI-MS and the MS/MS analyses of the unidentified products associate them to multiple isomers containing carboxylic acids, oxo-carboxylic acids and hydroxy-carbonyls functions. They also show that some of these reaction products can be assimilated to oligomers. The time profiles of these products point out that their formation can involve radical mechanisms. The ability of these compounds to produce SOA upon water droplets evaporation was, for the first time to our knowledge, experimentally examined by nebulizing and drying the reaction samples, in order to simulate a cloud evaporation process. The results clearly showed a significant production of SOA. A clear evolution of the particle size distributions with the reaction time was obtained: an increase of the aerosol mass from 0.03 $\mu g\,m^{-3}$ to 27.8 $\mu g\,m^{-3}$, within 22 h of reaction was observed. From these results, a SOA mass yield of 2–12% was determined. Our results have experimentally evidenced that cloud processes of methacrolein can produce, through photooxidation reactions, significant amounts of SOA. Finally, since methacrolein is one of the major oxidation products of isoprene, which is the main emitted VOC on the global scale, it can be anticipated that in-cloud processes can form significant amounts of SOA, which previously have not been taken into account for a global estimation of SOA atmospheric impacts. These SOA formation pathways should be further investigated to better understand the processes involved in the formation of low volatile products and the way they contribute to SOA formation. Moreover, in order to better evaluate the relevance of these processes in the production of SOA at a regional or global scale, further works are still needed, considering reaction conditions that compare to the real troposphere, in term of (i) reactants concentrations, (ii) aqueous phase reaction time, and (iii) composition of the clouds droplets (SVOCs and oxidants – such as NO_3, Cl, SO_4^-).

Acknowledgements. This study was funded by the French PN-LEFE-CHAT (Programme National-Les Enveloppes Fluides et l'Environnement-Chimie Atmosphérique), by the Provence-Alpes-Côte-d'Azur Region, and by the French ERICHE network.

Edited by: V. F. McNeill

References

Altieri, K. E., Carlton, A. G., Lim, H., Turpin, B. J., and Seitzinger, S. P.: Evidence for Oligomer Formation in Clouds: Reactions of Isoprene Oxidation Products. Environ. Sci. Technol., 40, 4956–4960, 2006.

Altieri, K. E., Seitzinger, S. P., Carlton, A. G., Turpin, B. J., Klein, G. C., and Marshall, A. G.: Oligomers formed through in-cloud methylglyoxal reactions: Chemical composition, properties, and mechanisms investigated by ultra-high resolution FT-ICR mass spectrometry, Atmos. Environ., 42, 1476–1490, 2008.

Blando, J. D. and Turpin, B. J.: Secondary organic aerosol formation in cloud and fog droplets: a literature evaluation of plausibility, Atmos. Environ., 34, 1623–1632, 2000.

Carlton, A. G., Turpin, B. J., Lim, H., Altieri, K. E., and Seitzinger, S.: Link between isoprene and secondary organic aerosol (SOA): pyruvic acid oxidation yields low volatility organic acids in clouds, Geophys. Res. Lett., 33, L06822/1–L06822/4, doi:10.1029/2005GL025374, 2006.

Carlton, A. G., Turpin, B. J., Altieri, K. E., Seitzinger, S., Reff, A., Lim, H., and Ervens, B.: Atmospheric oxalic acid and SOA production from glyoxal: Results of aqueous photooxidation experiments, Atmos. Environ., 41, 7588–7602, 2007.

Claeys, M., Graham, B., Vas, G., Wang, W., Vermeylen, R., Pashynska, V., Cafmeyer, J., Guyon, P., Andreae, M. O., Artaxo, P., and Maenhaut, W.: Formation of Secondary Organic Aerosols Through Photooxidation of Isoprene, Science (Washington DC, USA), 303, 1173–1176, 2004a

Claeys, M., Wang, W., Ion, A. C., Kourtchev, I., Gelencser, A., and Maenhaut, W.: Formation of secondary organic aerosols from isoprene and its gas-phase oxidation products through reaction with hydrogen peroxide, Atmos. Environ., 38, 4093–4098, 2004b.

Dommen, J., Metzger, A., Duplissy, J., Kalberer, M., Alfarra, M. R., Gascho, A., Weingartner, E., Prevot, A. S. H., Verheggen, B., and Baltensperger, U.: Laboratory observation of oligomers in the aerosol from isoprene/NO_x photooxidation, Geophys. Res. Lett., 33, L13805/1–L13805/5, doi:10.1029/2006GL026523, 2006.

Dron, J., Eyglunent, G., Temime-Roussel, B., Marchand, N., and Wortham, H.: Carboxylic acid functional group analysis using constant neutral loss scanning-mass spectrometry, Anal. Chim. Acta, 605, 61–69, 2007.

Edney, E. O., Kleindienst, T. E., Jaoui, M., Lewandowski, M., Offenberg, J. H., Wang, W., and Claeys, M.: Formation of 2-methyl tetrols and 2-methylglyceric acid in secondary organic aerosol from laboratory irradiated isoprene/NO_x/SO_2/air mixtures and their detection in ambient $PM_{2.5}$ samples collected in the eastern United States, Atmos. Environ., 39, 5281–5289, 2005.

Ervens, B., George, C., Williams, J. E., Buxton, G. V., Salmon, G. A., Bydder, M., Wilkinson, F., Dentener, F., Mirabel, P., Wolke, R., and Herrmann, H.: CAPRAM2.4 (MODAC mechanism): An extended and condensed tropospheric aqueous phase mechanism and its application, J. Geophys. Res., 108(D14), 4426, doi:10.1029/2002JD002202, 2003.

Ervens, B., Feingold, G., Frost, G. J., and Kreidenweis, S. M.: A modelling study of aqueous production of dicarboxylic acids, Part 1: Chemical pathways and organic mass production, J. Geophys. Res., 109, D15205, doi:10.1029/2003JD004387, 2004a.

Ervens, B., Feingold, G., Clegg, S. L., and Kreidenweis, S. M.: A modelling study of aqueous production of dicarboxylic acids, Part 2: Impact on cloud microphysics, J. Geophys. Res., 109, D15206, doi:10.1029/2003JD004575, 2004b.

Ervens, B., Carlton, A. G., Turpin, B. J., Altieri, K. E., Kreidensweis, S. M., and Feingold, G.: Secondary organic aerosol yields from cloud-processing of isoprene oxidation products, Geophys. Res. Lett., 35, L02816/1–L02816/5, doi:10.1029/2007GL031828, 2008.

Gelencsér, and Varga, Z.: Evaluation of the atmospheric significance of multiphase reactions in atmospheric secondary organic aerosol formation, Atmos. Chem. Phys., 5, 2823–2831, 2005, http://www.atmos-chem-phys.net/5/2823/2005/.

Guzmán, M. I., Colussi, A. I., and Hoffmann, M. R.: Photoinduced oligomerization of aqueous pyruvic acid, J. Phys. Chem. A, 110, 3619–3626, 2006.

Kanakidou, M., Seinfeld, J. H., Pandis, S. N., Barnes, I., Dentener, F. J., Facchini, M. C., Van Dingenen, R., Ervens, B., Nenes, A., Nielsen, C. J., Swietlicki, E., Putaud, J. P., Balkanski, Y., Fuzzi, S., Horth, J., Moortgat, G. K., Winterhalter, R., Myhre, C. E. L., Tsigaridis, K., Vignati, E., Stephanou, E. G., and Wilson, J.: Organic aerosol and global climate modelling: a review, Atmos. Chem. Phys., 5, 1053–1123, 2005, http://www.atmos-chem-phys.net/5/1053/2005/.

Kawamura, K. and Sakaguchi, F.: Molecular distributions of water soluble dicarboxylic acids in marine aerosols over the Pacific Ocean including tropics. J. Geophys. Res., 104(D3), 3501–3509, 1999.

Kroll, J. H., Ng, N. L., Murphy, S. M., Flagan, R. C., and Seinfeld, J. H.: Secondary Organic Aerosol Formation from Isoprene Photooxidation, Environ. Sci. Technol., 40, 1869–1877, 2006.

Lee, W., Baasandorj, M., Stevens P. S., and Hites, R. A.: Monitoring OH-Initiated Oxidation Kinetics of Isoprene and Its Products Using Online Mass Spectrometry, Environ. Sci. Technol., 39, 1030–1036, 2005.

Liao, H., Adams, P. J., Seinfeld, J. H., Mickley, L. J., and Jacob, D. J.: Interactions between tropospheric chemistry and aerosols in a unified GCM simulation, J. Geophys. Res., 108(D1), 4001, doi:10.1029/2001JD001260, 2003.

Lim H., Carlton A. G., and Turpin B. J.: Isoprene forms secondary organic aerosol through cloud processing: model simulations. Environ. Sci. Technol., 39, 4441–4446, 2005.

Liu, Yao, El Haddad, I., Scarfogliero, M., Nieto-Gligorovski, L., Temime-Roussel, B., Quivet, E., Marchand, N., Picquet-Varrault, B., and Monod, A.: In-cloud processes of methacrolein under simulated conditions – Part 1: Aqueous phase photooxidation, Atmos. Chem. Phys., 9, 5093–5105, 2009, http://www.atmos-chem-phys.net/9/5093/2009/.

Loeffler, K. W., Koehler, C. A., Paul, N. M., and De Haan, D. O.: Oligomer formation in evaporating aqueous glyoxal and methyl glyoxal solutions, Environ. Sci. Technol., 40, 6318–6323, 2006.

Michaud, V., El Haddad, I., Liu, Yao, Sellegri, K., Laj, P., Villani, P., Picard, D., Marchand, N., and Monod, A.: In-cloud processes of methacrolein under simulated conditions – Part 3: Hygroscopic and volatility properties of the formed secondary organic aerosol, Atmos. Chem. Phys., 9, 5119–5130, 2009, http://www.atmos-chem-phys.net/9/5119/2009/.

Monod, A., Chebbi, A., Durand-Jolibois, R., and Carlier, P.: Oxidation of methanol by hydroxyl radicals in aqueous solution under simulated cloud droplet conditions, Atmos. Environ., 34, 5283–5294, 2000.

Müller, J.-F., Stavrakou, T., Wallens, S., De Smedt, I., Van Roozendael, M., Potosnak, M. J., Rinne, J., Munger, B., Goldstein, A., and Guenther, A. B.: Global isoprene emissions estimated using MEGAN, ECMWF analyses and a detailed canopy environment model, Atmos. Chem. Phys., 8, 1329–1341, 2008, http://www.atmos-chem-phys.net/8/1329/2008/.

Paulsen, D., Weingartner, E., Alfarra, M. R., and Baltensperger, U.: Volatility measurements of photochemically and nebulizer-generated organic aerosol particles, J. Aerosol Sci., 37, 1025–1051, 2006.

Poulain, L., Monod, A., and Wortham, H.: Development of a new on-line mass spectrometer to study the reactivity of soluble organic compounds in the aqueous phase under tropospheric conditions: Application to OH-oxidation of N-methylpyrrolidone, J. Photoch. Photobio. A, 187, 10–23, 2007.

Sempere, R. and Kawamura, K.: Low molecular weight dicarboxylic acids and related polar compounds in the remote marine rain samples collected from western Pacific, Atmos. Environ., 30, 1609–1619, 1996.

Sokal, R. R. and Rohlf, F. J.: Biometry, 2 ed., Freeman, New York, USA, 1981.

Surratt, J. D., Murphy, S. M., Kroll, J. H., Ng, N. L., Hildebrandt, L., Sorooshian, A., Szmigielski, R., Vermeylen, R., Maenhaut, W., Claeys, M., Flagan, R. C., and Seinfeld, J. H.: Chemical Composition of Secondary Organic Aerosol Formed from the Photooxidation of Isoprene, J. Phys. Chem. A, 110, 9665–9690, 2006.

van Pinxteren, D., Plewka, A., Hofmann, D., Mueller, K.; Kramberger, H., Svrcina, B., Baechmann, K., Jaeschke, W., Mertes, S., Collett, J. L., and Herrmann, H.: Schmuecke hill cap cloud and valley stations aerosol characterisation during FEBUKO (II): Organic compounds, Atmos. Environ., 39, 4305–4320, 2005.